

Received: 2018.01.31  
Accepted: 2018.03.22  
Published: 2018.04.29

# Imaging-Assisted Diagnosis and Characteristics of Suspected Spinal Brucellosis: A Retrospective Study of 72 Cases

Authors' Contribution:  
Study Design A  
Data Collection B  
Statistical Analysis C  
Data Interpretation D  
Manuscript Preparation E  
Literature Search F  
Funds Collection G

DE **Laiyong Tu**  
BC **Xinmei Liu**  
BF **Wenfei Gu**  
FG **Zhenbin Wang**  
BD **Zhenfeng Liu**  
BD **Enfeng Zhang**  
BE **Aikenmu Kahar**  
CF **Ge Chu**  
AE **Jiang Zhao**

Department of Spinal Surgery, Traditional Chinese Medicine Hospital of Xinjiang Uygur Autonomous Region, Urumchi, Xinjiang, P.R. China

**Corresponding Author:** Jiang Zhao, e-mail: xjzhaojiang@163.com  
**Source of support:** Natural Science Foundation of the Xinjiang Uygur Autonomous Region (2015211C153)

**Background:** We clarified the imaging features of *Brucella* spondylitis to enhance our understanding of the disease and to minimize misdiagnosis.


**Material/Methods:** Imaging data (X-ray, computed tomography [CT], and magnetic resonance imaging [MRI] data) of 72 *Brucella* spondylitis patients treated from 2010 to 2017 were retrospectively analyzed; diagnoses was made by evaluating laboratory and pathological data.

**Results:** X-ray films revealed changes in intervertebral space heights, the number of lateral osteophytes, and bone destruction, which were more severe in the following order: lumbosacral vertebrae (56 cases, 77.8%), cervical spine (6 cases, 8.3%), thoracic spine (5 cases, 6.9%), and multi-segmental mixed vertebrae (5 cases, 6.9%). CT revealed osteolytic destruction attributable to early-stage *Brucella* spondylitis (endplate and vertebral lamellar osteolysis), usually associated with multiple vertebral involvement, with the middle and late disease stages being characterized by osteophytes in the vertebral margins and bony bridges, endplate sclerosis, and vertebral osteosynthesis. We encountered 54 cases (75%) with endplate lamellar osteolysis, 37 (51.4%) with vertebral lamellar osteolysis, 59 (81.9%) with marginal osteophytes, 10 (13.9%) with bony bridges, 25 (34.7%) with vertebral laminar sclerosis, and 17 (23.6%) with vertebral osteosynthesis. MRI revealed early, low-intensity, differential T1WI vertebral and intervertebral signals, with occasional iso-signals, T2WI iso-signals or high-intensity signals; and T2WI-FS vertebral and intervertebral high-intensity signals, commonly from vertebral soft tissues and rarely from paravertebral abscesses.

**Conclusions:** A better understanding of the X-ray, CT, and MRI features of *Brucella* spondylitis could aid in diagnosis when combined with epidemiological and laboratory data, thus minimizing misdiagnosis.

**MeSH Keywords:** **Brucella • Brucellosis • Spine**

**Full-text PDF:** <https://www.medscimonit.com/abstract/index/idArt/909288>

 2421

 2

 6

 34



## Background

Brucellosis, also known as Mediterranean retention, Maltese fever, or heat wave, is a zoonotic allergic disease caused by *Brucella* that can trigger epidemics that seriously endanger the health of humans and animals. Over 170 countries or regions worldwide have reported human and animal epidemics [1–5]. Over 500 000 people worldwide develop brucellosis annually [6]. Among animals, cattle, pigs and, especially, sheep are most affected [7–9]. The Chinese “Animal Epidemic Prevention Act” recognizes brucellosis as a Type 2 infectious disease that can cause significant economic loss; strict control and eradication measures are mandated to prevent proliferation [10].

In 2015 and 2016, we visited pastoral areas in northern Xinjiang, Uygur Autonomous Region, to epidemiologically investigate brucellosis, and found that the prevalence rates were 8.4% and 25%, respectively. In recent years, increasing numbers of brucellosis outbreaks in livestock have been reported in the Xinjiang Uygur Autonomous Region, seriously affecting the local economy and the health of local residents. Brucellosis remains an important public health problem.

The major pathological feature of *Brucella spondylitis* is nodular lesions consisting of epithelioid cells, which can be seen in the nidus under a light microscope. Affected areas may show histiocytosis, proliferative nodules, and granuloma, as well as large numbers of neutrophils, lymphocytes, monocytes, and eosinophils. The typical mechanism of brucellosis infection is direct contact with the skin or mucosa, although infection can also occur via inhalation of airborne droplets into the respiratory tract. Brucellosis can also invade the spine; this occurs in 2–53% of cases [11–13]. The disease can involve any part of the spine, but lumbar and thoracic/lumbar involvement is most common, affecting the lumbosacral and sciatic nerve roots, radiating pain into the lower limbs, and causing meningitis; spinal inflammation; spinal arachnoid (afternoon) fever; hyperhidrosis; limb aches, numbness, and weakness; paraplegia; and other problems that seriously affect quality-of-life and impose large economic burdens on society [14–18]. In the early stage of brucellosis, the clinical manifestations are nonspecific. Relatively common symptoms include undulant fever, sweating, exhaustion, and poor appetite. If the nerve root or spinal cord is affected, leg weakness may occur, in addition to chronic pain and swelling of the lymph nodes, liver, or spleen. In patients with acute brucellosis, the morphology of the infected vertebrae is normal. The endplates, which have a rich blood supply, are the first vertebral bodies to be affected. Inflammation eventually spreads to the entire vertebral body, accompanied by early vertebral infections wherein inflammatory congestion and edema are the principal pathological changes, in addition to increased amounts of water in the vertebral bodies. However, no obvious spinal deformities or bone destruction

attributable to changes in the vertebral morphology are evident. When the disease enters its subacute and chronic stages, immune cells interact with the infected foci and bone destruction occurs. Infected vertebral bodies undergo complex changes, including hyperosteogenesis and sclerosis. Thus, the signal intensities of vertebral bodies are uneven, even when osteoporosis in diseased vertebrae and obvious changes in vertebral body morphology are absent. The clinical and imaging manifestations are very similar to those of spinal tuberculosis, including narrowing of vertebral gaps, destruction of vertebral bodies, formation of bony bridges, and widening of the shadow of the vertebral column [19,20]. Cases with delayed or aggravated illness caused by early clinical misdiagnosis are frequent [21].

We retrospectively analyzed data on 72 cases of spinal brucellosis treated in our hospital. We summarized and analyzed imaging manifestations and diagnostic points to improve diagnosis and reduce misdiagnosis.

## Material and Methods

### General information

Inclusion criteria were: (1) a reliable diagnosis of spinal brucellosis, and a complete and clear set of clinical images; and, (2) voluntary participation in the study and signed written informed consent. Exclusion criteria were: (1) a previous diagnosis of ankylosing spondylitis; (2) a relapse of spinal brucellosis; (3) previous spinal surgery; (4) any spinal deformity, such as scoliosis; (5) poor image quality or positioning; (6) a clinical diagnosis of spinal tuberculosis; and (7) tuberculosis patients. The imaging data (X-ray, computed tomography [CT], and magnetic resonance imaging [MRI]) of the 72 included patients treated from January 2010 to January 2017 were collected, of whom 53 were males and 19 females, ages 30–77 years (average, 52.0 years). The time since diagnosis was 1–6 months (average, 3.7 months). All patients had been in an epidemic area or in contact with pathogenic bacteria. The specimens of all the patients were collected postoperatively for pathological examination, with the results revealing chronic suppurative inflammation in all cases. Forty-five patients (62.5%) were engaged in animal husbandry and 22 (30.6%) in beef/mutton slaughter and processing, and 5 (6.9%) lived in brucellosis-endemic regions. The T-SPOT tuberculosis test was positive in all patients, as was at least 1 of the Rose Bengal plate and tube agglutination tests.

### Imaging

All 3 imaging examinations were performed at about the same time (the interval between CT and MRI did not exceed 15 days). If pedicle involvement was suspected, the double oblique position

was added to routine X-ray radiography. Spiral CT images were obtained of all lesions of vertebral bodies and adjacent vertebrae (layer thickness 4–5 mm, pitch 1–1.5, both bony and soft tissue window displays). Conventional MRI was performed using Phillips 0.5-T and Siemens 1.5-T platforms (fitted with spinal coils) in the sagittal plane (spin echo and fast spin echo sequences), followed by axial and coronal T2WI (T1WI TR/TE 500 ms/20 ms; T2WI TR/TE 4,000 ms/120 ms; FOV 300, layer thickness 4–5 mm, slice thickness 1 mm, no row enhancement).

## Observations

Using the same optical conditions, X-ray, CT, and MRI images with quality scores  $\geq 3$  were independently evaluated by 3 doctors in terms of clinical manifestations, bone destruction (as revealed by MRI), skeletal sclerosis, dead bone and abscess formation, calcification, intervertebral disc destruction, changes in the heights of intervertebral spaces, vertebral canal involvement, posterior axonal deformities, and surrounding soft-tissue changes.

## Results

### X-ray performance

The main manifestations of acute spinal brucellosis were the involvement of multiple vertebral bodies, multiple lesions, irregular insect-like bone destruction, and (later) hyperplasia, sclerosis, and spur formation. Bone destruction was not obvious on X-rays, but lesions were found in vertebral bodies and/or endplates (Figures 1, 2). The lumbosacral vertebrae were the most commonly involved (56 cases, 77.8%), followed by 6 cases (8.3%) of cervical spine involvement, 5 (6.9%) of thoracic spine involvement, and 5 (6.9%) of multiple-segment vertebral body involvement (Table 1). A total of 53 patients exhibited 1–2 involved vertebral bodies and 19 exhibited  $\geq 3$  involved vertebral bodies. Wedge-shaped changes (10 cases) were less common. Intervertebral space changes  $>50\%$  were apparent in 44 cases (61.1%) and changes  $<50\%$  in 21 (29.2%). Fifty-five cases exhibited lateral osteophytes (76.4%)

### CT imaging

The CT imaging features were divided into those of the vertebral osteolysis and vertebral hyperplastic sclerosis stages. CT revealed early osteolytic destruction (dissolution of endplate and vertebral lamellar bone), (usually) multiple vertebral body involvement, and some osteophyte-mediated destruction. Later, proliferative sclerosis of the vertebral bodies, with osteophyte proliferation, bony bridge formation, endplate sclerosis, and vertebral osteoporosis, were apparent. In general, most bone destruction foci at vertebral edges were small and

multiple; the hyperplastic and sclerotic foci were more obvious; and sites of new bone formation and new foci of destruction were admixed. Disc and synovial cartilage destruction exhibited an isodense pattern as hyperplasia of the articular surface advanced and the density of the adjacent vertebral body increased (Figure 3, 4). In terms of osteolytic destruction, 54 cases (75%) exhibited endplate lamellar and 37 (51.4%) exhibited vertebral body lamellar dissolution. Fifty-nine cases had marginal osteophytes (81.9%); bony bridge formation was evident in 10 (13.9%); vertebral lamellar sclerosis in 25 (34.7%); and osteogenesis within the vertebrae in 17 (23.6%; Table 2).

### MRI

The typical MRI T1WI manifestation was low- or iso-signal intensity in areas of bone destruction. T2WI was associated with high- or iso-signal intensity, and lipid suppression with high signal intensity. Peripheral bone sclerosis was associated with low T1WI and T2WI signals; and soft tissue with low T1WI and high- or iso-signal T2WI signals. In terms of intervertebral disc involvement, intervertebral space stenosis yielded uneven signals and vertebral abscesses evident in coronal scans were “teardrop-shaped” (Figures 5, 6). In 67 cases (93.1%) with involved vertebral bodies and 57 with involved intervertebral discs (79.2%), most signals were of low intensity; high- (2.7%, 13.9%) and iso-signal-intensity signals (4.2%, 6.9%) were less common. T2WI signals from involved vertebral bodies were usually high- (40 cases, 55.6%) or iso-signal (21 cases, 29.2%) intensity; affected intervertebral discs yielded high (30 cases, 41.7%) or low (22 cases, 30.6%) signals. Sixty-eight (94.4%) affected vertebral bodies and 64 (88.9%) affected intervertebral discs yielded high-intensity signals in the fat-suppressed phase. Paravertebral soft-tissue shadows were evident in 40 cases (55.6%), predural granulomas in 26 (36.1%), and paravertebral abscesses in 6 (8.3%).

## Discussion

Spinal brucellosis remains an important complication of brucellosis worldwide, and early diagnosis is critical [22–24]. In the acute phase, X-rays reveal the involvement of multiple vertebral bodies and multiple bony lesions [25,26]. We found that the lumbosacral vertebrae were most commonly involved (56 cases, 77.8%), followed by cervical, thoracic, and multiple vertebral bodies (5 cases of the latter, 6.9%). Fifty-three cases (73.7%) exhibited 1–2 involved vertebral bodies. We found that bone destruction was not evident on X-rays, especially in those with early-stage disease. Later, the centers of vertebral bodies may become invaded and harden, preventing deep bone destruction. Later imaging manifestations included hyperplasia, sclerosis, and bony spines resembling “bird beaks” (that sometimes formed bony bridges). Wedge-shaped changes

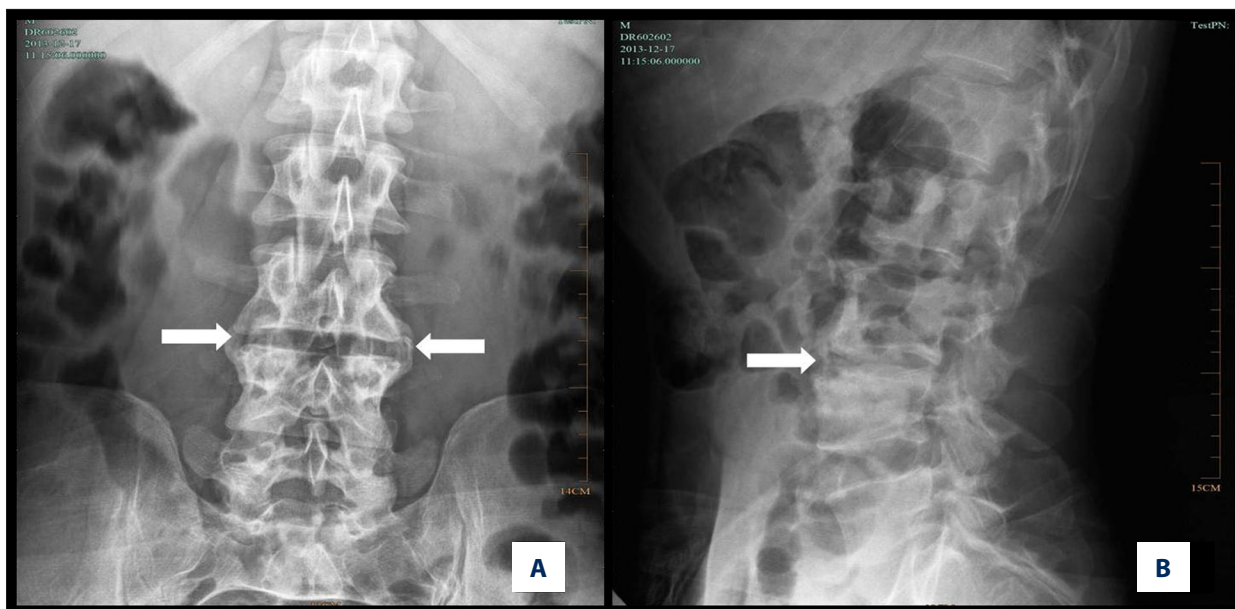


**Figure 1.** X-ray results of a male patient aged 39 years with spinal brucellosis. Anteroposterior (A) and lateral (B) X-rays reveal lesions in the L3/4 vertebral bodies, visible bilateral hyperplasia of the vertebral bone, stenosis of the intervertebral space, and a belt of endplate and vertebral body sclerosis (white arrows).

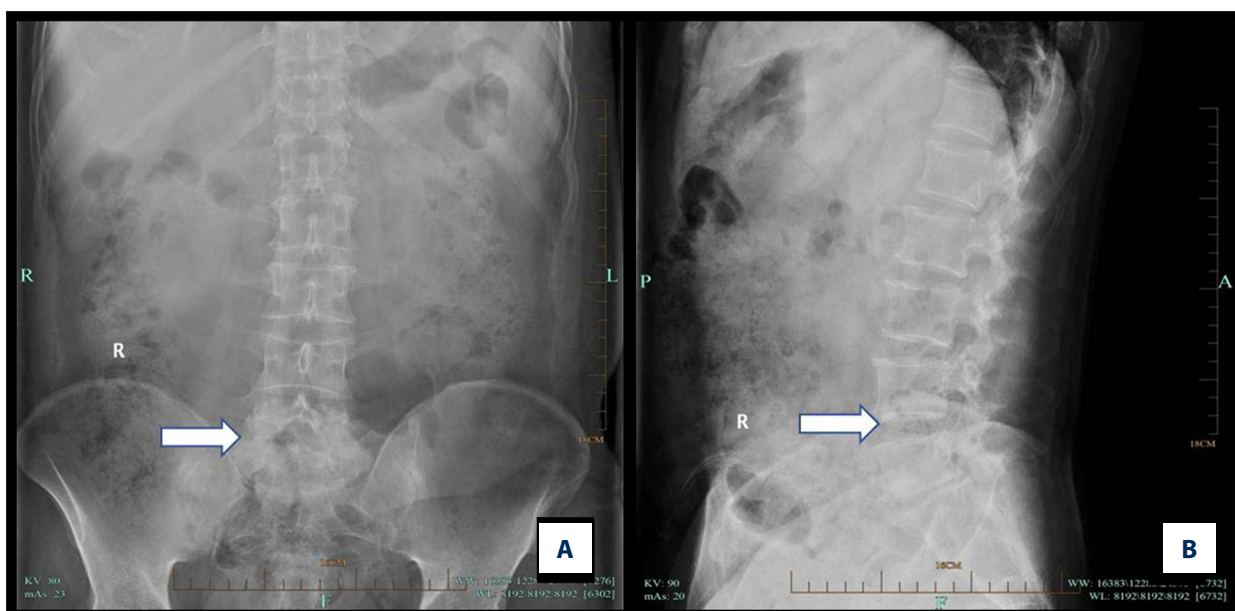


**Figure 2.** X-ray results of a male patient aged 52 years with spinal brucellosis. Anteroposterior (A) and lateral (B) X-rays reveal lesions in the L5-S1 vertebral bodies, visible bilateral hyperplasia of vertebral bone, stenosis of the intervertebral space, and a belt of endplate and vertebral body sclerosis (white arrows).

**Table 1.** Locations of the lesions.

	Cervical vertebra	Thoracic vertebra	Lumbosacral vertebra	Multiple cervical locations
Number	6/72	5/72	56/72	5/72
Percentage	8.3%	6.9%	77.8%	6.9%

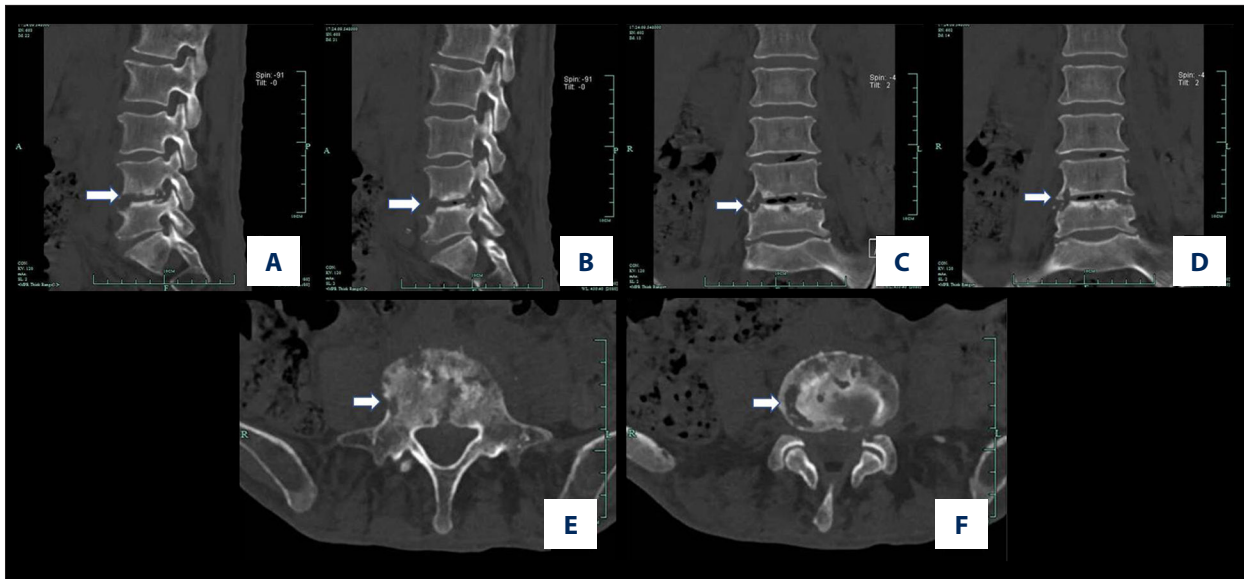


**Figure 3.** Computed tomography (CT) results of a male patient aged 77 years with spinal brucellosis. Sagittal (A, B) and coronal (C, D) images reveal vertebral body lesions at the L4/5 level. The lower endplate of the L4 vertebral body, as well as the L5 upper endplate and vertebral body, exhibit bony destruction with bilateral, and vertebral body bridge formation. The L4/5 endplate also shows denaturalization, while the vertebral body shows osteogenesis (white arrows). Axial view (E, F) revealing osteolytic destruction of the vertebral body (white arrows).

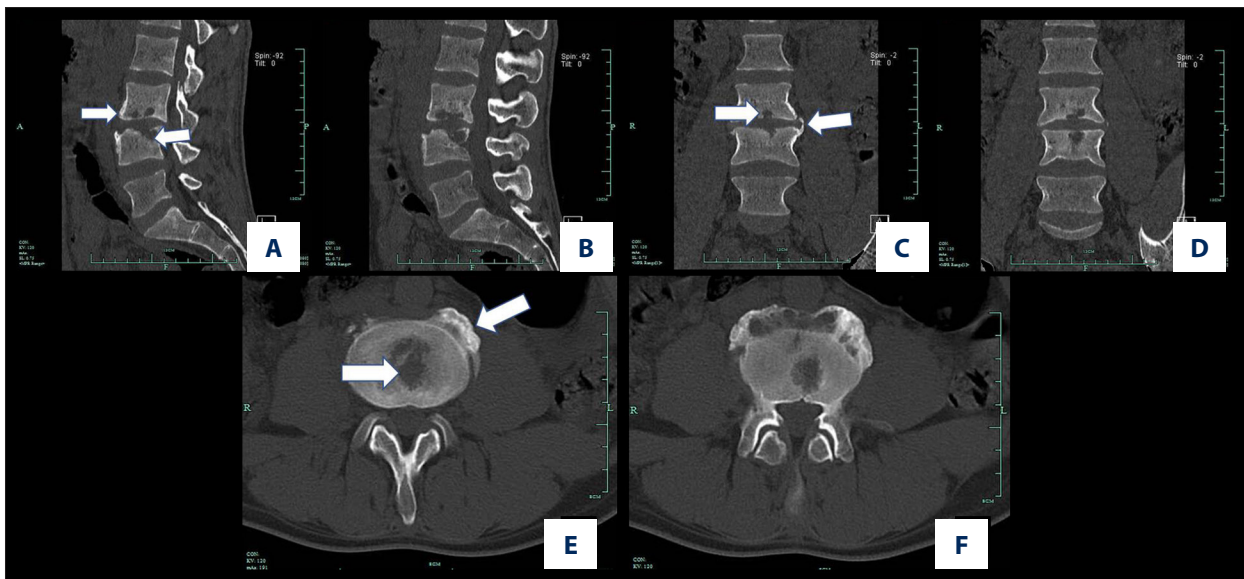


**Figure 4.** CT results of a male patient aged 39 years with spinal brucellosis. Sagittal (A, B) and coronal (C, D) images revealing vertebral body lesions at the L3/4 level. The lower endplate of the L3 vertebral body and the L4 upper endplate and vertebral body exhibit bony destruction with bilateral, vertebral, bony bridge formation, as well as L3/4 endplate denaturalization and vertebral body osteogenesis (white arrows). Axial image (E, F) revealing osteolytic destruction of the vertebral body (white arrows).

in vertebral bodies were rare and intervertebral space changes were more common (although seldom reported in previous studies). Fifty-five cases had lateral bony masses (76.4%), bone destruction was not obvious and vertebral bodies and/or endplates in affected areas exhibited hardening.

The CT characteristics of the disease may be divided into those associated with vertebral bone destruction and vertebroplastic sclerosis. The disease has been divided into an acute period (2–3 months), a subacute period (3–12 months), and a chronic period (>12 months). The early CT manifestations in patients

**Table 2.** CT imaging features by lesion stage.

		Number	Percentage
Osteolytic destruction	Endplate lamellar dissolution	54	75.0%
	Vertebral body lamellar dissolution	37	51.4%
Hyperosteoegeny	Marginal osteophytes	59	81.9%
	Bony bridge formation	10	13.9%
	Vertebral laminar sclerosis	25	34.7%
	Osteogenesis within the vertebra	17	23.6%

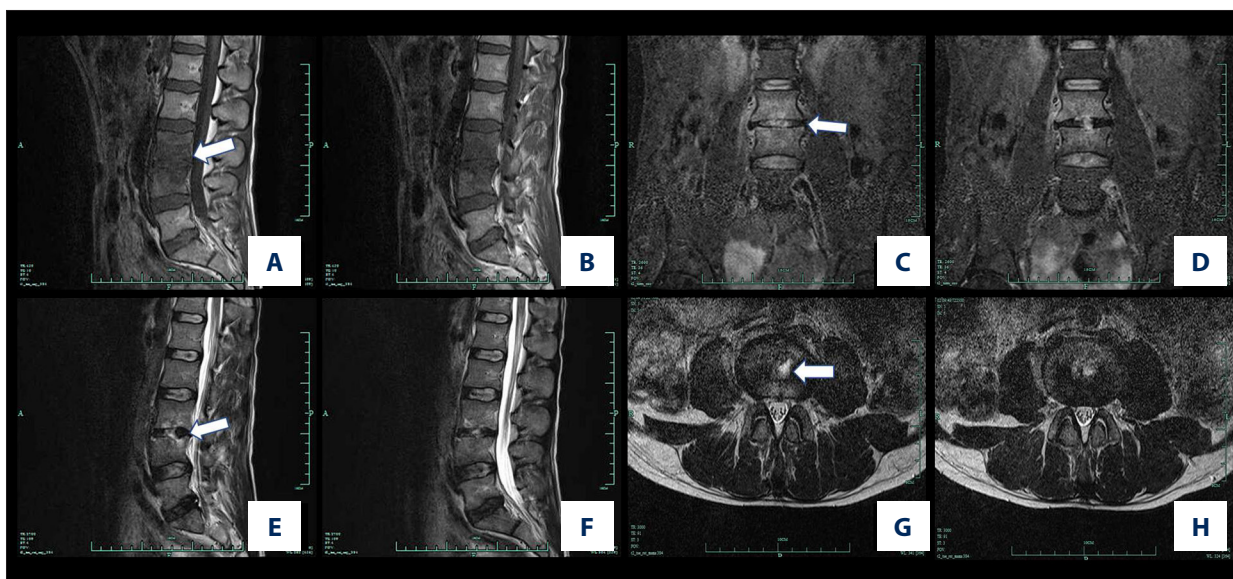


**Figure 5.** Magnetic resonance imaging (MRI) results of a male patient aged 39 years with spinal brucellosis. The lesion was located at the L3/4 vertebrae. T1WI imaging of the vertebral body and low-level signaling from the intervertebral disc (A, B). On the T2WI images, the vertebral body and intervertebral disc exhibit high- and low-intensity signals, respectively (C, D), while the T2WI-FS images reveal high-intensity signals from the vertebral body and intervertebral disc (E, F). A teardrop-shaped abscess is also evident in the axial image (G, H). White arrows show the position of the lesion.

with osteolysis (endplate and vertebral lamellar bony dissolution) usually have multiple vertebral body involvement and low-level osteophyte-mediated bone destruction. The principal CT features in the sclerotic period are vertebral body hyperplasia, osteophyte proliferation, bony bridge formation, endplate sclerosis, and vertebral body osteogenesis [19]. Demirci et al. [27] reported an unusual “cauliflower” sign on vertebral CT of a patient with spinal brucellosis; this sign may be disease-specific.

We found 54 cases (75%) of lamellar osteolysis, 37 (51.4%) of vertebral lamellar bone dissolution, 59 (81.9%) of marginal osteophyte status, 10 (13.9%) of bony bridge formation, 25 (34.7%) of laminar sclerosis, and 17 (23.6%) of vertebral body osteogenesis. In general, manifestations of bone destruction at the vertebral edges of lesions were both small and multiple; lesions around the hyperplastic and sclerotic regions were

more obvious. New bone tissue was mixed with the new lesion, destruction of the intervertebral disc and synovial cartilage yielded isodense images, the articular surfaces were both hyperplastic and sclerotic, and the bone densities of adjacent vertebrae were increased. Earlier studies showed negative vertebral body CT manifestations in the destruction planes associated with bilateral lumbar muscle widening, often accompanied by abscess formation [15,16,28–30]. However, we found only a few paravertebral abscesses on CT and further study is required.

MRI is very sensitive to changes in amount of water in tissue and protein and reveals destruction of vertebral body bone and the intervertebral discs, and abscesses within and outside the vertebral canal. In patients with early-stage disease, MRI sensitively detects changes in vertebral bodies and

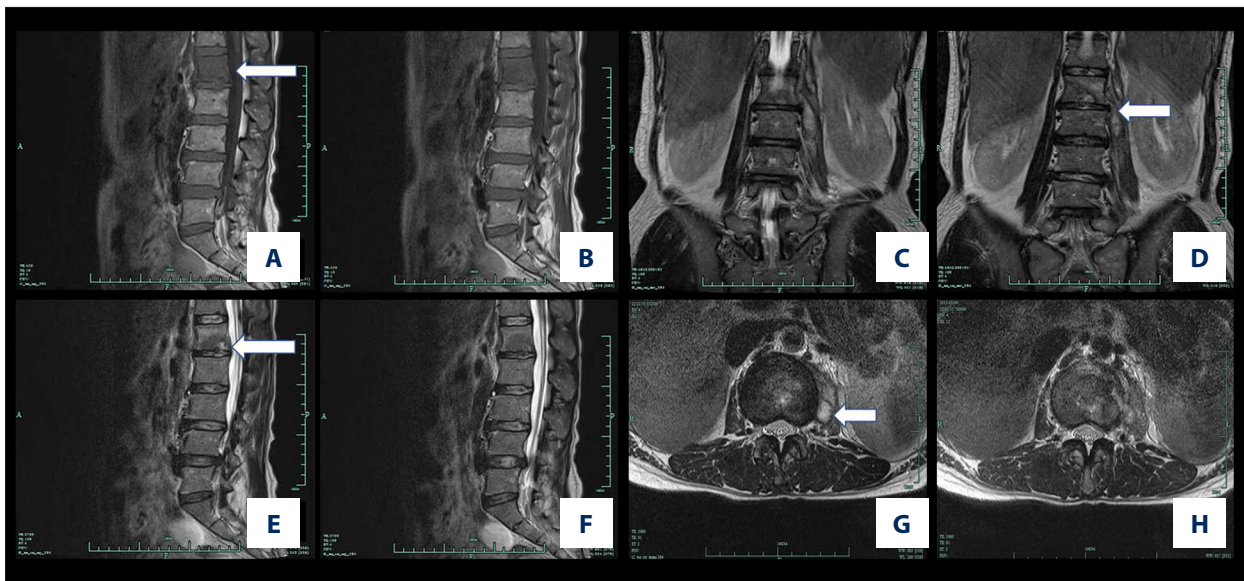


**Figure 6.** The MRI results of a female patient aged 41 years with spinal brucellosis. The lesion is located at the L1/2 vertebrae. T1WI images of the vertebral body reveal low-intensity signals from the intervertebral disc (A, B). On the T2WI scans, the vertebral body and intervertebral disc exhibit high- or low-level mixed signals (C, D), and the T2WI-FS scans exhibit high-intensity signals from the vertebral body and intervertebral disc (E, F). A teardrop-shaped abscess is also evident in the axial image (G, H).

surrounding soft tissue. Typically, MRI signals from regions experiencing peripheral bone sclerosis are either unaffected or reduced on T1WI, unaffected or elevated on T2WI, or reduced on both T1WI and T2WI. Soft-tissue involvement reduces the T1WI signal, either does not affect or elevates the T2WI signal, and is associated with MRI-inferred intervertebral disc involvement or intervertebral space narrowing via a reduction in signal non-uniformity [31,32]. We found that the T1WI signals from both the vertebral body and the intervertebral disc were commonly of low intensity; signals of high or mixed intensity were rare. On T2WI, an affected vertebral body delivered either a normal or high signal, as did the intervertebral disc. The fat-phase signals from the vertebrae and intervertebral discs were high. Paraspinal soft tissue shadows and predural granulomas were more common than usual, and paravertebral abscesses were less common. Also, paravertebral abscesses evident on MRI coronal scans were “teardrop-shaped,” a feature rarely reported before. As MRI can detect early abnormal signals from vertebral bodies, intervertebral discs, and soft tissue, this is the first-choice imaging when evaluating patients with spinal brucellosis, and enhanced MRI scans improve diagnostic accuracy.

The imaging features of spinal brucellosis need to be distinguished from those of spinal tuberculosis. The incidence of spinal tuberculosis can attain 40–50%, being the most common manifestation of pulmonary tuberculosis, often triggering vertebral body destruction and other serious complications. The clinical and imaging manifestations are very similar to those

of brucellosis spondylitis, making misdiagnosis easy. The typical manifestations of spinal tuberculosis are bone destruction, dead bone, narrow intervertebral spaces, paraspinal abscesses, and deformities of the spinal posterior process. Spinal spondylitic brucellosis often involves the endplates of the junctions between the vertebral bodies and the intervertebral discs. The shape of the vertebral body is not affected, the posterior process does not exhibit compression or deformity, no bony hyperplasia is evident at the edges of vertebral bodies, bone death is rare, the intervertebral spaces are not obviously narrowed in those with early-stage disease, abscesses in the vertebrae and the psoas major muscle are rare, and abscess heterogeneity is limited. In general, only adjacent vertebrae are affected, the vertebral bodies suffer only minor destruction, and adjacent organs are not involved [33]. Our imaging data for patients with brucellosis spondylitis support these findings. Differential diagnosis requires the evaluation of biopsy samples. Furthermore, brucellosis titer test positivity and anti-brucellosis positivity are useful diagnostic criteria [34]. Clinicians, especially orthopedic surgeons, must understand the disease, particularly the imaging features, to allow accurate diagnosis via a combination of epidemiological history-taking, clinical manifestations, and laboratory data.

## Conclusions

In summary, brucellosis is easily misdiagnosed, although it is important to achieve an early diagnosis to prevent further

complications. Blood cultures and *Brucella spondylitis* serology tests are required when patients with spinal lesions do not respond to standard treatment. The features of *Brucella spondylitis* in X-ray, CT, and MR images must also be better understood to minimize misdiagnosis and to use in combination with epidemiological and laboratory data.

## References:

- Liu ZG, Di DD, Wang M et al: *In vitro* antimicrobial susceptibility testing of human *Brucella melitensis* isolates from Ulanqab of Inner Mongolia, China. *BMC Infect Dis*, 2018; 18: 43
- Asakura S, Makingi G, Kazwala R, Makita K: Brucellosis risk in urban and agro-pastoral areas in Tanzania. *Ecohealth*, 2018 [Epub ahead of print]
- Justman N, Fruchtmann Y, Greenberg D, Shalom BS: Hematologic manifestations of brucellosis in children. *Pediatr Infect Dis J*, 2018 [Epub ahead of print]
- Al-Griw HH, Kraim ES, Farhat ME et al: Evidence of ongoing brucellosis in livestock animals in North West Libya. *J Epidemiol Glob Health*, 2017; 7(4): 285–88
- Mailybayeva A, Yespembetov B, Ryskeldinova S et al: Improved influenza viral vector based *Brucella abortus* vaccine induces robust B and T-cell responses and protection against *Brucella melitensis* infection in pregnant sheep and goats. *PLoS One*, 2017; 12: e0186484
- Franc KA, Krecek RC, Hasler BN, Arenas-Gamboa AM: Brucellosis remains a neglected disease in the developing world: A call for interdisciplinary action. *BMC Public Health*, 2018; 18: 125
- Lopez GE, Pena S, Escobar GI et al: Serological study of brucellosis in Argentine Creole sheep. *Rev Argent Microbiol*, 2018 [Epub ahead of print]
- Alhamada AG, Habib I, Barnes A, Robertson I: Risk factors associated with brucella seropositivity in sheep and goats in Duhok Province, Iraq. *Vet Sci*, 2017; 4(4): pii: E65
- Sonekar CP, Kale S, Bhojar S et al: Brucellosis in migratory sheep flock from Maharashtra, India. *Trop Anim Health Prod*, 2018; 50: 91–96
- Zhou L, Fan M, Hou Q et al: Transmission dynamics and optimal control of brucellosis in Inner Mongolia of China. *Math Biosci Eng*, 2018; 15(2): 543–67
- Applebaum GD, Mathisen G: Spinal brucellosis in a southern California resident. *West J Med*, 1997; 166(1): 61–65
- Chelli Bouaziz M, Ladeb MF, Chakroun M, Chaabane S: Spinal brucellosis: A review. *Skeletal Radiol*, 2008; 37: 785–90
- Turgut M, Turgut AT, Kosar U: Spinal brucellosis: Turkish experience based on 452 cases published during the last century. *Acta Neurochir (Wien)*, 2006; 148(10): 1033–44; discussion 1044
- Tali ET, Koc AM, Oner AY: Spinal brucellosis. *Neuroimaging Clin North Am*, 2015; 25: 233–45
- Ates O, Cayli SR, Kocak A et al: Spinal epidural abscess caused by brucellosis. Two case reports. *Neurol Med Chir*, 2005; 45: 66–70
- Boyaci A, Boyaci N, Tutoglu A, Dokumaci DS: Spinal epidural abscess in brucellosis. *BMJ Case Rep*, 2013; 2013: pii: bcr2013200946
- Coskun E, Suzer T, Yalcin N, Tahta K: Spinal extradural compression caused by granuloma of brucellosis. *Scand J Infect Dis*, 1998; 30: 311–13
- Sankaran-Kutty M, Marwah S, Kutty MK: The skeletal manifestations of brucellosis. *Int Orthop*, 1991; 15: 17–19
- Arslan F, Karagoz E, Arslan BY et al: Spinal brucellosis diagnosed with positron emission tomography combined with computed tomography (PET/CT). *Spine J*, 2016; 16: e381–82
- Zhao YT, Yang JS, Liu TJ et al: Sclerosing vertebra in the spine: Typical sign of spinal brucellosis. *Spine J*, 2015; 15: 550–51
- Alp E, Doganay M: Current therapeutic strategy in spinal brucellosis. *Int J Infect Dis*, 2008; 12: 573–77
- Arkun R, Mete BD: Musculoskeletal brucellosis. *Semin Musculoskelet Radiol*, 2011; 15: 470–79
- Zaks N, Sukenik S, Alkan M et al: Musculoskeletal manifestations of brucellosis: A study of 90 cases in Israel. *Semin Arthritis Rheum*, 1995; 25: 97–102
- al-Shahed MS, Sharif HS, Haddad MC et al: Imaging features of musculoskeletal brucellosis. *Radiographics*, 1994; 14: 333–48
- Tekkok IH, Berker M, Ozcan OE et al: Brucellosis of the spine. *Neurosurgery*, 1993; 33: 838–44
- Iqbal QM, Khan O: Brucellosis of the spine. *J R Coll Surg Edinb*, 1990; 35: 395–97
- Demirci M, Tan E, Durguner M et al: Spinal brucellosis. A case with “cauliflower” appearance on CT. *Neuroradiology*, 1989; 31: 282–83
- Zhang Q, Yang X, Yu H et al: Spinal epidural abscess caused by *Brucella* species: A review of 17 cases. *J Neurosurg Sci*, 2017; 61: 271–76
- Hu T, Wu J, Zheng C, Wu D: Brucellar spondylodiscitis with rapidly progressive spinal epidural abscess showing cauda equina syndrome. *Spinal Cord Ser Cases*, 2016; 2: 15030
- Starakis I, Solomou K, Konstantinou D, Karatza C: Brucellosis presenting as a spinal epidural abscess in a 41-year-old farmer: A case report. *Cases J*, 2009; 2: 7614
- Yang X, Zhang Q, Guo X: Value of magnetic resonance imaging in brucellar spondylodiscitis. *Radiol Med*, 2014; 119(12): 928–33
- Bozgeyik Z, Aglamis S, Bozdag PG, Denk A: Magnetic resonance imaging findings of musculoskeletal brucellosis. *Clin Imaging*, 2014; 38: 719–23
- Erdem H, Elaldi N, Batirel A et al: Comparison of brucellar and tuberculous spondylodiscitis patients: results of the multicenter “Backbone-1 Study”. *Spine J*, 2015; 15: 2509–17
- Yasar K, Pehlivanoglu F, Cicek G, Sengoz G: The evaluation of the clinical, laboratory and the radiological findings of the fifty-five cases diagnosed with tuberculous, Brucellar and pyogenic spondylodiscitis. *J Neurosci Rural Pract*, 2012; 3: 17–20

## Conflict of interest

None.